JTTEE5 6:463-468

Zirconium Boride and Tantalum Carbide Coatings Sprayed by Electrothermal Explosion of Powders

H. Tamura, M. Konoue, and A.B. Sawaoka

(Submitted 26 October 1996; in revised form 18 February 1997)

Refractory zirconium diboride and tantalum monocarbide ceramic powders were sprayed using an electrothermal explosion caused by a high-voltage electric breakdown and large-current discharge heating. This spray technique was improved using a purpose-designed powder container, which made it possible to melt the powder completely and accelerate it to impinge on substrates. The electrical energy applied to the powder was estimated to be about twice the energy theoretically needed to melt just the powder.

Although the ceramics used in this work are hard-sintered materials by nature, they could be sprayed and deposited to form coatings on metal substrates without additives and sintering agents. The coatings formed exhibited no chemical decomposition in the boride, and only small amounts of decarburization in the carbide due to its nonstoichiometry. The tantalum carbide coating mixed with iron and aluminum substrates in the range of 10 μm to several tens of micrometers.

Keywords coating microstructure, electrothermal explosion, tantalum carbide, zirconium boride

1. Introduction

Spray coatings of refractory metals and ceramics have been used in the fabrication of energy equipment, including gas-turbine engines, nuclear reactors, magnetohydrodynamic power generators, and steel-production equipment—all of which are operated under high-temperature conditions to enhance their performance. Increasing the operating temperature to accommodate higher performance requirements in the future will require coatings with improved properties.

Some advanced ceramics exhibit excellent intrinsic properties without sintering agents. Although some refractory carbides, borides, and nitrides with high melting points and hardness can be used as fine ceramic coatings with heat and wear resistance, these materials usually are sprayed as cermets to suppress their oxidation and/or decomposition and to enhance interparticle bonding and adhesion to substrates. Under higher-temperature conditions, however, cermets lose heat resistance due to melting of their metallic component. This calls for development of a new method of spraying fine nonoxide ceramics with no additives, as well as examination of their properties as a tough coating under severe physical and chemical circumstances.

This paper characterizes a new technique for the spraying of zirconium boride and tantalum carbide coatings without additives. Although the principles of this technique have been described previously (Ref 1), the present method results in improved spraying of refractory ceramic powders.

H. Tamura, M. Konoue, and **A.B. Sawaoka,** Materials and Structures Laboratory, Tokyo Institute of Technology, Nagatsuta 4259, Midori-ku, Yokohama 226, Japan.

2. Description of Spray Method

The technique uses powder particles of electrically conductive materials. The powder is charged into an electrically insulating tube, the ends of which are plugged with refractory tungsten electrodes. The tube is then connected to a pair of electrical contacts set in a steel chamber and is electrically broken down by the application of a high voltage through the contacts, resulting in Joule (I^2R) heating of the powder particles and an explosion due to the high current discharge.

This explosion of powder is different from the heating process and electrical discharge used with thin wires of conductive bulk material in conventional exploding wire spray techniques (Ref 2, 3). Since the powder naturally includes some gas, which is electrically insulating, it initially has a high resistance at the onset of the electrical discharge. In addition, heating of the powder contained in the insulating tube is independent of the ambient atmosphere even during the final stage of the discharge. Heating of a bare wire, by contrast, is characterized by good initial conductance and depends on the pressure that allows other current paths to be established at the onset of vaporization of the wire.

Here, two kinds of powders, zirconium diboride (ZrB_2) and tantalum monocarbide (TaC), were sprayed by the electrothermal explosion technique. Tantalum monocarbide has the highest melting point (approximately 4150 to 4270 K) of all the inorganic materials (Ref 4-6). Enhancement of the mechanical strength of the insulating tube allowed the TaC to be sprayed. The spraying of ZrB_2 does not necessitate such stringent containment conditions, because this powder has a lower melting point of 3300 K (Ref 4).

3. Experimental Setup

The powder prepared for this technique was packed in a specially designed container concentrically composed of an inner polyethylene insulating tube and an outer cylindrical copper jacket (Fig. 1). The jacket, which fit over the insulating tube, had an outer diameter of 14 mm, a length of 50 mm, and a window that measured 4 mm wide by 40 mm long. The ZrB_2 powder (CERAC Co., Ltd., USA) had an average particle size of 10 μm or smaller and a purity of 99.5%; the TaC powder (Kojundo Chemical Laboratory Co., Ltd., Japan) had a particle size of 2 to 4 μm and a purity of 99.5%. The powder was charged into the tube under argon gas at atmospheric pressure (1.013×10^5 Pa).

The powder container was connected to the electrical contacts in a cylindrical vacuum chamber, and the contacts were connected to the electrical circuit. A 500 μF capacitor supplied high voltages and high currents to the powder. Molten particles produced by electrical heating of the powder were ejected from the tube through the jacket window during the electrothermal explosion. A substrate holder that faced the window (Fig. 1) was positioned at a standoff distance of 80 mm from the container axis. Each 2 mm thick substrate had a surface dimension of 10×10 mm^2 and was polished to a mirrorlike finish.

The voltage applied between the tungsten electrodes was estimated from measurements using a high-voltage probe (Model HV-P30, Iwatsu Co., Japan) connected to the electrical contacts of the chamber and a Rogowski coil to detect current flow in the powder (Ref 1). The micromorphology of sprayed deposits was observed with an electron probe microanalyzer (EPMA) (Model EPMA-1400, Shimadzu Co., Japan), and the crystal structure was determined using an x-ray diffraction (XRD) analyzer (Model M18XHF, Mac Science, Japan). Vickers microhardness was measured with a hardness tester (Model MVK-EIII, Akashi Seisakusho, Ltd., Japan).

4. Experimental Results and Discussion

4.1 *Heating of ZrB_2 Powder*

A low-density (0.91×10^3 kg/m^3) polyethylene tube with outer and inner diameters of 5 and 3 mm, respectively, was used to spray the ZrB_2 powder. The tube was packed to 50 mm with the powder at a relative density of 53.4%. The powder container was set in the vacuum chamber filled with dry air at a pressure of 6.7×10^3 Pa. After the capacitor was charged to 8.4 kV, high voltage was applied to the powder to cause an electrical breakdown.

Figure 2(a) shows waveforms of the voltage applied to the outer electric contacts of the chamber and of the discharge current flowing in the powder container. The time origin was the moment of trigger-signal output to the discharge circuit. The electrical breakdown occurred at 65 μs after the voltage was applied.

To estimate the time-varying apparent resistance of the powder, the voltage produced by multiplication of the chamber inductance and the time differential of the discharge current was subtracted from the voltage measured by the high-voltage probe. The voltage directly applied to the powder container thus was calculated and used with the measured current to estimate the apparent resistance, as shown in Fig. 2(b). In addition, the Joule heating of the powder was evaluated from the electric power—calculated from the apparent resistance and discharge current. According to the resistivity of tungsten as a function of temperature (Ref 4), the resistance of the tungsten electrodes would correspond to a maximum of 5% of the apparent resistance. Thus, the power shown in Fig. 2(c) was believed to be used to heat the powder.

The electrothermal explosion of conductive powders is characterized by the resistance characteristics. As shown in Fig. 2(b), the resistance decreased from an initial value greater than 10 Ω to about 0.04 Ω. After the resistance remained at this value for about 20 μs, it decreased again. This second decrease is indicated by arrow β in Fig. 2(b) and was thought to be due to (1) the discharge lasting in the low-resistive plasma region left inside the container after ejection of a large amount of hot powder particles with high resistivity or (2) the generation of other electrical paths in the reduced gas pressure region outside the powder container. The latter phenomenon has been described previously in Ref 1, and such electrical paths would be formed through the hot gas and plasma ejecting from the window of the powder container.

Once the second decrease of the resistance has occurred, proper evaluation of the energy consumption in the powder particles is impossible. The energy consumption in the powder was thus calculated to be approximately 11 kJ by time integrating the power (Fig. 2c) until the second decrease in resistance. This value corresponded to approximately 270% of the energy, 4.0 kJ, needed to heat the ZrB_2 powder particles alone to their melting point. The values of specific heat and heat of fusion used for ZrB_2 were C_p (J/kg · K) $= 5.52 \times 10^2 + 1.67 \times 10^{-1}\ T - 1.55 \times 10^7\ T^{-2}$ and E_f (J/kg) $= 9.30 \times 10^5$ (Ref 4), respectively, where T is temperature.

4.2 *Heating of TaC Powder*

The TaC powder was charged to 50 mm in a high-density (0.94×10^3 kg/m^3) polyethylene tube with outer and inner diameters of 6 and 3 mm, respectively. The tensile strength of this

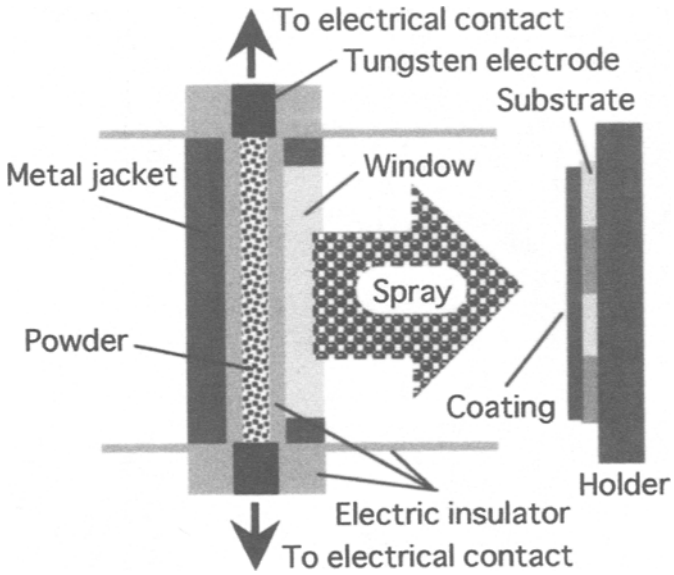

Fig. 1 Cross-sectional schematic of the container holding ceramic powder

tube was estimated to be about six times greater than the one used for the ZrB_2 powder. The relative density of the powder packed in the tube was 46.4%.

The applied voltage, discharge current, and apparent resistance of the TaC powder are shown as a function of time in Fig. 3(a) and (b). The electric power was also estimated (Fig. 3c). The energy consumption was calculated to be about 9 kJ during the 70 μs pulse, which corresponded to 190% of the energy, 4.7 kJ, needed to melt the powder alone with no other losses, where the specific heat and heat of fusion used for TaC were C_p (J/kg · K) = $2.24 \times 10^2 + 5.88 \times 10^{-2} T - 4.56 \times 10^6 T^{-2}$ and E_f (J/kg) = 5.44×10^5, respectively (Ref 4).

4.3 *Powder Heating Behavior*

The starting powders used were originally composed of particles of conductive materials and argon gas. The particles contacted together only through microspots, and the interparticle space was filled with the electrically insulating argon gas. In addition, the particle surface became oxidized, providing further electrical insulation. Therefore, the powder must have high resistance at the initial stage of the electric discharge. However, this resistance will decrease due to the heat accompanying the increase in conductivity of the argon gas and plasma and of the contact area of the particles. This agrees with the exponential decrease of the apparent resistance shown in Fig. 2(b) and 3(b).

Further heating of the powder particles, however, causes an increase in resistance as a function of temperature, and the apparent resistance should then decrease slowly. The plateaus on the curves in Fig. 2(b) and 3(b) are believed to correspond to this further heating of the particles. As described earlier, the ejection of high-resistive powder particles and low-resistive gas from the container at its break would be followed by the establishment of a low-resistive electrical discharge path inside or outside the container. The onset of such discharge thus caused the second steep decrease in resistance. Although the slight decrease, indicated by arrow α in Fig. 2(b) and 3(b), was also observed on the resistance curve prior to the plateau and may have been due to

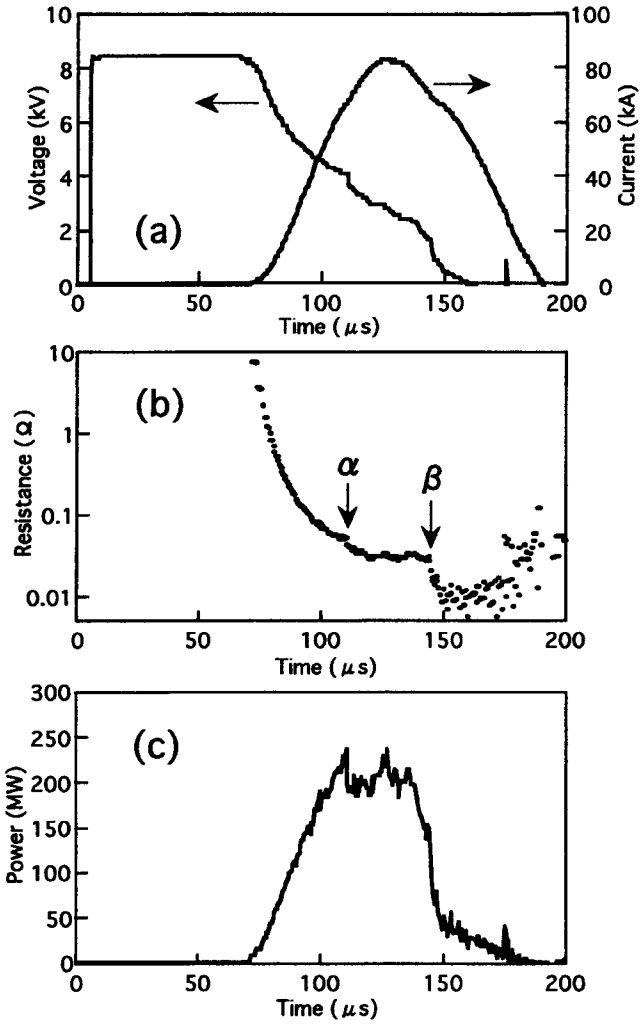

Fig. 2 Waveforms of voltage and current (a) applied to the electrical contacts of a vacuum chamber holding a ZrB_2 powder container. Also shown are the apparent resistance of the powder (b) and the electric power applied (c).

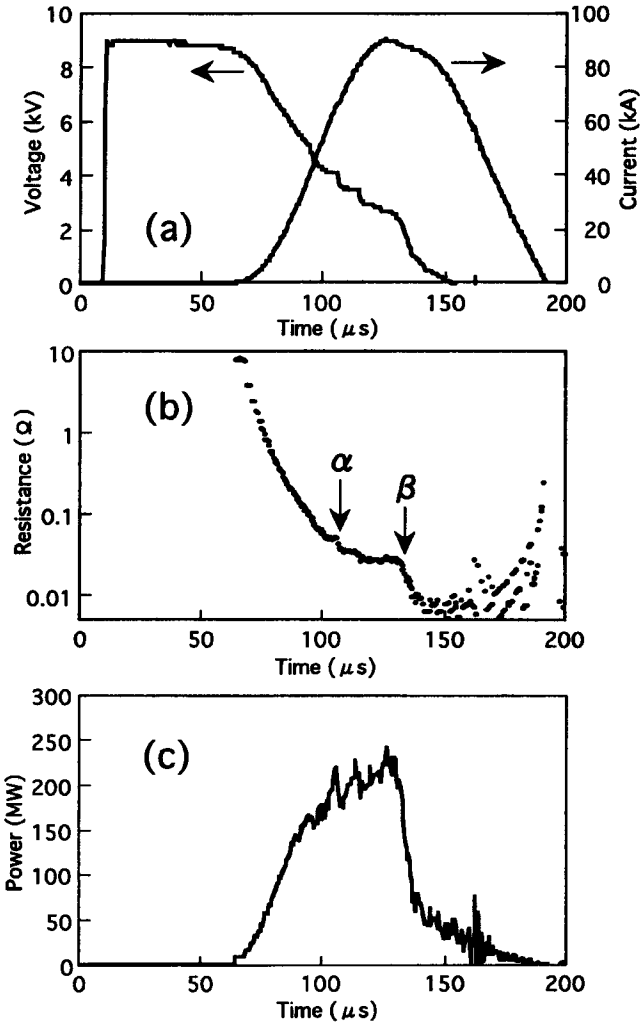

Fig. 3 Waveforms of voltage and current (a) applied to the electrical contacts of a vacuum chamber holding a TaC powder container. Also shown are the apparent resistance of the powder (b) and the electric power applied (c).

ejection of a small amount of heated particles having high resistivity, this should not have been large enough to initiate the other current paths outside the tube.

The electric energy supplied in the powder was estimated from the time-integration of the power up to the onset of the second steep decrease in resistance. This energy was larger than that required to melt the powder alone. The energy calculated above, therefore, should be divided among the acceleration of molten particles, breakup of the tube and deformation of the metal jacket, and melting of the powder.

4.4 *Coating Characterization*

The results of EPMA characterization of the ZrB_2 and TaC coating morphologies are shown in Fig. 4(a) and (b), respectively. Analysis by XRD revealed that these coatings were composed of only ZrB_2 or TaC_x. Spherical or rounded surfaces are visible in Fig. 4. No angular starting particles were found. Thus, it is hypothesized that the coatings were produced by deformation and solidification of molten spherical particles impacting on the substrates.

The crystal structure of ZrB_2 is known to be hexagonal, of the AlB_2 type, with lattice constants of 3.168 and 3.528 Å, on the *a*-axis and *c*-axis, respectively (Ref 5). The lattice constants of the starting powder were measured to be 3.1672 ± 0.0004 Å and 3.5257 ± 0.0013 Å on the *a*-axis and *c*-axis, respectively. The XRD spectra from the ZrB_2 coating contained peaks for ZrB_2 only, and the lattice parameters of the *a*- and *c*-axes were estimated to be 3.1683 ± 0.0004 Å and 3.5288 ± 0.0011 Å, respectively.

The crystal structure of TaC_x is known to be cubic, of the NaCl type, while its nonstoichiometry varies over the range $0.6 < x < 0.99$ (Ref 6). The change in stoichiometry corresponds to that of the lattice constant. The lattice constant of $TaC_{0.99}$ is known to be 4.4555 Å (Ref 6), and that of the starting powder was measured to be 4.4535 ± 0.0002 Å. The XRD spectra from the top surface of the TaC coating on a mild steel substrate were observed over the range of 2θ between 70° and 130°, and were analyzed with respect to its lattice constant. No other secondary crystal phases (e.g., tantalum, TaC_2, or crystalline carbon) were detected, but tantalum carbides of the general formula TaC_x were found. The lattice constant was calculated to be 4.4367 ± 0.0002 Å, corresponding to a carbon content, *X*, of approximately 0.87, with no effect of impurities on the lattice.

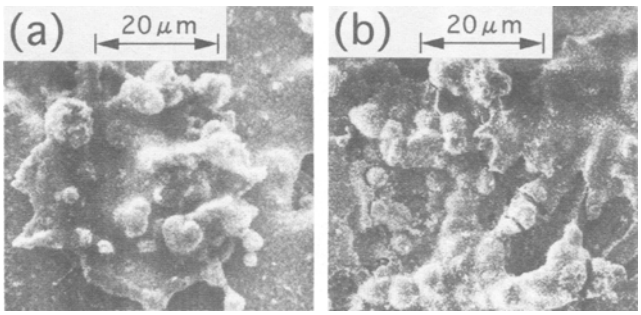

Fig. 4 Scanning electron microscope (SEM) images of coating top surfaces. (a) ZrB_2. (b) TaC

Scanning electron images of cross sections of the ZrB_2 coating on mild steel and aluminum substrates are shown in Fig. 5(a) and (d), respectively. The element maps for zirconium and iron are shown in Fig. 5(b) and (c), respectively. The relative amounts of the elements present are indicated by the 14 colors, graded from red (highest) to purple (lowest). Comparison of the SEM images to the element maps revealed the thickness of these coatings to be about 20 to 30 μm. Since no lamellar structure was found in either coating, it appears that the coatings were formed via high-density deposition and solidification of molten particles. These maps also showed that the interface between the ZrB_2 coating and the steel substrate was smooth, as was the initial substrate, and that the ZrB_2 was distributed across the interface, overlapping due to mixing to a depth of approximately 5 μm.

The Vickers microhardness of the cross section of the ZrB_2 coating on the mild steel substrate was measured to be 19.3 ± 2.1 GPa for a 50 gf load applied for 10 s; the microhardness of bulk ZrB_2 is known to be 22 GPa (Ref 5). The material interface on the aluminum substrate was observed by comparing the element maps of zirconium and aluminum (Fig. 5e and f, respectively) and was in the range of about 5 μm.

The SEM image of the cross section of the TaC coating on a mild steel substrate is shown in Fig. 5(g), next to element maps of tantalum and iron (Fig. 5h and i, respectively). Comparison of the image with the tantalum map indicates the area of the TaC ceramic layer, since XRD analysis showed only that the coating consisted of tantalum carbide. The iron map showed an uneven interface between the substrate and the TaC coating; whereas the starting substrate exhibited a smooth surface. It was also found that the TaC layer mixed with the substrate to a depth of several micrometers to 10 μm.

The Vickers microhardness measured on this TaC coating layer on mild steel was 11.8 ± 1.7 GPa with a 10 gf load and a loading time of 10 s; the microhardness of bulk $TaC_{0.99}$ is known to be 17 GPa (Ref 5). It was thought that the distribution of the steel in the ceramic coating resulted in the relatively low hardness.

The TaC coating on an aluminum substrate (Fig. 5j) was characterized by heavy mixing of the TaC with the substrate. The mixing is shown in the element maps of Fig. 5(k) and (l). The aluminum appeared even on the top surface of the TaC coating in the range of 50 μm, while the tantalum concentration decreased gradually toward the substrate. Although the TaC coating on the aluminum substrate did not always cover with such heavy mixing of the materials, the mixing range was much larger than that on the iron substrate and the ZrB_2 coat made on aluminum. Since the melting point and heat capacity per unit volume of aluminum are, respectively, 1.9 and approximately 1.5 to 1.7 (for $T = 373$ to 773 K, for instance) times smaller than those of mild steel, the melted zone of the aluminum substrate might be larger than that of the steel substrate due to heat transition from the coating material. In addition, since aluminum has (1) a density of 2.69×10^3 kg/m^3, (2) a shock impedance of 17.3×10^6 N · s/m^3 (given by multiplication of the density and bulk sound velocity), and (3) a microhardness of 0.4 GPa (with a 50 gf load), and since these three properties are approximately 34, 37, and 28%, respectively, of those of mild steel, then the driving force of material mixing at the interface should work more effectively on the aluminum substrate.

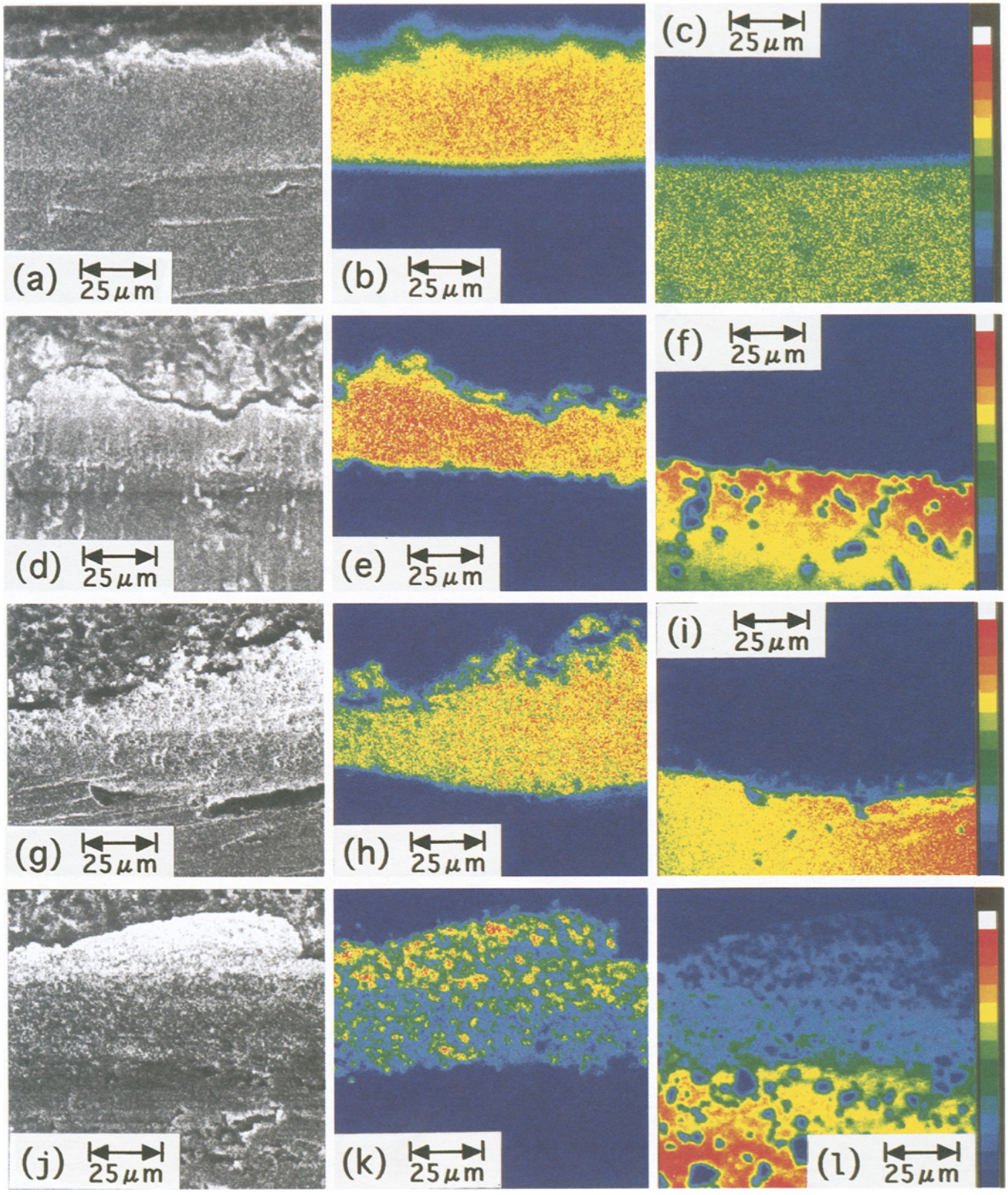

Fig. 5 (a) SEM image of cross section of ZrB_2 coating formed on mild steel substrate. (b) Zirconium element map on mild steel substrate. (c) Iron element map. (d) SEM image of cross section of ZrB_2 coating formed on aluminum substrate. (e) Zirconium element map on aluminum substrate. (f) Aluminum element map. (g) SEM image of cross section of TaC coating formed on mild steel substrate. (h) Tantalum element map on mild steel substrate. (i) Iron element map. (j) SEM image of cross section of TaC coating formed on aluminum substrate. (k) Tantalum element map on aluminum substrate. (l) Aluminum element map. Note: The relative amounts of the elements present are indicated by the 14 colors, graded from red (highest) to purple (lowest).

5. Conclusions

Powder spray coatings of ZrB_2 and TaC were produced by the electrothermal explosion technique. A specially designed powder container allowed electric energies to be supplied which could be twice the melting energy of the powder. Molten particles ejected from the container formed deposits through deformation and solidification during impingement on a substrate.

The resulting coatings were characterized by an interface between the deposited layer and the substrate. When TaC was sprayed onto the soft aluminum with a relatively low melting point, the mixing of these materials was more than 50 μm. Thus, significant interaction of materials across the interface can be expected for materials used in this spray process.

The TaC coating exhibited small change in chemical composition due to decarburization. However, highly refractory ceramics were sprayed and deposited to form a ceramic coating on metal substrates without the use of additives or sintering agents to suppress chemical decomposition and enhance particle bonding.

Acknowledgments

This work was supported by a Grant-in-Aid for Scientific Research [(c)-07805066] of the Ministry of Education, Science, and Culture. The authors would like to thank Yoshinori Ikeda and Takatori Soda for their assistance in the measurements.

References

1. H. Tamura, M. Nagahama, Y. Tanabe, and A.B. Sawaoka, Spraying of Zirconium-Diboride Powder by an Electrical Column Explosion Technique and Its Mechanism, *J. Appl. Phys.*, Vol 75, 1994, p 4695-4703
2. T. Suhara, K. Kitajima, and S. Fukuda, The Structure and Adhesion of Coatings Deposited by Wire Explosion Spraying, *J. Vac. Sci. Technol.*, Vol 4, 1974, p 787-792
3. H. Tamura, T. Ogura, M. Nagahama, Y. Tanabe, and A.B. Sawaoka, Spraying of the Brittle Ceramic Zirconium Diboride by a Wire Explosion Technique, *J. Appl. Phys.*, Vol 75, 1994, p 1789-1797
4. R.B. Kontel'nikov, S.N. Basl'ikov, Z.G. Galiakbarov, and A.I. Kastanov, Ed., *High Refractory Elements and Compounds*, Nissotsuushinnsha, Wakayama, 1977, p 14, 15, 28, 30, 55, 221 (in Japanese)
5. G.V. Samsonov and I.M. Vinitskii, Ed., *Handbook of Refractory Compounds*, IFI/Plenum, 1980, p 40, 162, 292, 295
6. E.K. Storms, in *The Refractory Carbides*, J.L. Margrave, Ed., Academic Press, 1967, p 84, 93